Energy Reports 7 (2021) 3090–3098

Contents lists available at ScienceDirect

Energy Reports

journal homepage: www.elsevier.com/locate/egyr

Research paper

Application of artificial neural networks and fuzzy logics to estimate porosity for Asmari formation

Xiao Li [a,*], Bingxian Wang [b], Qiuyuan Hu [a], Lis M. Yapanto [c], Angelina Olegovna Zekiy [d]

[a] College of Oil and Gas Engineering, Shandong Institute of Petroleum and Chemical Technology, Dongying, Shandong, 257061, China
[b] Sinopec Petroleum Engineering Corporation, Dongying, Shandong, 257000, China
[c] Department of Aquatic Management, Faculty of Fisheries and Marine Science, Universitas Negeri Gorontalo, Indonesia
[d] Department of Prosthetic Dentistry, Sechenov First Moscow State Medical University, Moscow, Russia

ARTICLE INFO

Article history:
Received 13 April 2021
Received in revised form 10 May 2021
Accepted 20 May 2021
Available online 2 June 2021

Keywords:
Porosity estimation
Artificial neural network
Fuzzy logic
Asmari formation
Well logging tests

ABSTRACT

Porosity estimation is one of the essential issues in petroleum industries to distinguish the reservoir characteristics properly. Therefore, it is of importance to predict porosity with the optimum way to reduce the logging tests. In this study, artificial neural network and fuzzy logics are considered efficient techniques to predict the Asmari formation's porosity. The results of porosity estimation by intelligent neuro-phase method showed the ability of this method to estimate in complex conditions in Mansouri oilfield. Preparing data before training the neural network increases the power of the network in recognizing the appropriate pattern. In estimating the porosity in the Asmari reservoir of Mansouri field, gamma, acoustic, neutron and density and diameter measurements have a more influential role. Selecting the appropriate architecture for the neuro-phase network is effective in achieving more accurate results. This architecture includes selecting the type and number of membership functions for the inputs and the training algorithm with the appropriate number of iteration steps. The best estimation results by assigning four Gaussian membership functions to gamma image data, two Gaussian membership functions to each of the audio and neutron data, and three Gaussian membership functions to density image data and creating 40 laws in the data space. Inputs were obtained using a hybrid training algorithm. The average error of estimating porosity by the neuro-phase method in well C of Mansouri field is 1.28% in the validation data set, representing a correlation coefficient of 92.5% between the porosity extracted from the fuzzy neuro-fuzzy network and the porosity of the core.

© 2021 The Authors. Published by Elsevier Ltd. This is an open access article under the CC BY-NC-ND license (http://creativecommons.org/licenses/by-nc-nd/4.0/).

1. Introduction

Artificial neural networks are considered efficient and prosperous methods applied in various industries to perform a suitable application instead of implementing experimental evaluations (He et al., 2018a,b; Cheng et al., 2016; Chen et al., 2018, 2017; Kazemi and Yang, 2021, 2019; Zarra et al., 2019; Sharma and Garg, 2020; Davarpanah et al., 2018; Abasi et al., 2015, 2020; Huang et al., 2021b; Yang et al., 2020a; Yin et al., 2021). The function of artificial neural networks is based on the study of activities that take place in the human mind (Zuo et al., 2015, 2017; Yang et al., 2015; Ma et al., 2021; Xue et al., 2020; Najafi et al., 2013, 2012; Lee et al., 2019; Wawrzyniak, 2020; Davarpanah and Mirshekari, 2019a; Karbakhshzadeh et al., 2021b,a; Nan et al., 2021; Rostami et al., 2021). This method includes observational interpretation, summarization and learning (Jiang et al., 2018; Zhang et al., 2021; Yang et al., 2020b,a; Xu et al., 2021; Kargar et al., 2020; Rezaee et al., 2017; Valipour et al., 2012; Davarpanah, 2018b). Unlike previous methods that use a simple algorithm to solve specific problems, artificial neural networks use a sample-based method and usually perform a nonlinear survey between input and output data to solve problems (Mao et al., 2019; Huang and Ge, 2020; Zheng et al., 2021a,b; Huang et al., 2020b; Lin et al., 2020; Chen et al., 2021; Kartavykh et al., 2020; Wang et al., 2021; Hu et al., 2020; Hassanpour et al., 2021; Huang et al., 2021d; Huang and Wang, 2021; Zhang et al., 2020b; Yang et al., 2020b,a). Neural networks can determine the amount of field porosity using well graph data regardless of the limitations associated with the number of drilled wells (Zhang et al., 2020a; Li et al., 2017, 2019, 2020; Lim, 2005; Mazarei et al., 2019; Davarpanah and Mirshekari, 2019d; Zhang et al., 2020a; Huang et al., 2020a, 2021c). Despite their remarkable accuracy in approximating continuous functions, artificial neural networks do not provide users with any knowledge of the fitted model. Besides, in cases where there is uncertainty in the data or results, a low-confidence approximation of the fitted model is unexpected (Lim, 2005; Aggoun et al., 2006; Davarpanah, 2018a; Rabbani et al., 2018; Davarpanah,

* Corresponding author.
E-mail address: lixiao1022@126.com (X. Li).

https://doi.org/10.1016/j.egyr.2021.05.034
2352-4847/© 2021 The Authors. Published by Elsevier Ltd. This is an open access article under the CC BY-NC-ND license (http://creativecommons.org/licenses/by-nc-nd/4.0/).

2020; Davarpanah et al., 2019c,a; Gholami and Ansari, 2017; Huang et al., 2021a,e; Daryayehsalameh et al., 2021). Researchers in recent years have also used the theory of fuzzy logic to approximate continuous functions. This theory is the theory of fuzzy sets, which is itself an extension of the theory of sets with Boolean logic (Davarpanah et al., 2019b; Awan et al., 2020; Bafkar, 2020; Pan et al., 2020; Davarpanah and Mirshekari, 2020, 2019b, 2018; Esfandyari et al., 2020b; Ahmadi et al., 2014; Movahhed et al., 2019; Ebadi et al., 2020; Jalali Sarvestani and Charehjou, 2021; Maina et al., 2020). This theory provides a good basis for decision-making in inaccurate and ambiguous situations by attributing membership functions to training data, but few training algorithms are for these systems (Davarpanah, 2019; Ebadati et al., 2019b; Sun et al., 2020; Zhu et al., 2020; Davarpanah and Mirshekari, 2019c; Esfandyari et al., 2020a; Shokir, 2006). Intelligent techniques are very powerful tools that have found many applications in the oil industry. The reasons related to this can be stated as follows (Jafarinezhad and Shahbazian, 2015; Baouche and Aïfa, 2017; Nnaemeka, 2020; Nwankwo et al., 2020; Qayyum et al., 2020; Sepahvand et al., 2021a);

- These methods can process data quickly and have the ability to apply a built-in model to the system.
- These techniques are data-independent models that do not require prior knowledge of the data to which they are applied.
- Smart grids can accurately estimate the data they have been trained using existing datasets and their internal settings.
- Intelligent techniques can detect hidden non-linear relationships between data and, in this regard, especially for use in heterogeneous cases, including oil reservoirs.
- Given appropriate descriptive data, intelligent techniques produce a fast and reliable prediction at a speed that appears to be a new set of data for model construction (Wang et al., 2019; Aïfa et al., 2014; Ghiasi-Freez et al., 2014).

Zhou et al. (1993) used neural network methods to estimate porosity in an oil field in Canada based on acoustic and density neutron and gamma data. In this study, a four-layer neural network was designed for estimation. Its results on experimental wells showed that with the increasing complexity of geological conditions and cases where data other than experimental wells are given to the network, the network's ability to estimate decreases (Zhou et al., 1993). Elsharkawy (1998) introduced a new technique for modelling crude oil and natural gas systems' behaviour using a neural network model with a radial basis function. The model could predict the volume coefficient of oil formation, the ratio of soluble gas to oil, oil viscosity. They used the PVT data of the step-by-step release test of 90 samples to train the network model and ten other samples to test the model. The results showed a more accurate estimation of the mentioned parameters based on the artificial neural network than experimental relations (Elsharkawy, 1998). Singh (2005) used artificial neural networks to estimate permeability based on gamma-ray and neutron graph data and density in Utah Field in the Gulf of Uinta. In this study, data from seven wells were used as educational data and data from six wells were used as experimental data. The results obtained from the neural network proved the remarkable ability of this method in estimation (Singh, 2005; Ebadati et al., 2019a).

Lim (2005) used the combined neuro-phase method to estimate the permeability and porosity of reservoir rock based on well logs in Korea's oil fields. In this study, fuzzy curves were first used to extract the best images related to porosity and permeability. Then the neural network method was used to create a suitable estimation function between inputs and outputs. Based on the fuzzy curves, the best porosity-related images were short-range resistance (LLS), long-range resistance (LLD), neutron and density images, and the best permeability-related images were acoustic images, respectively. Density, gamma, neutron and potential were spontaneous. Based on these logs and in one of the wells of this field, porosity and permeability were estimated with acceptable accuracy, and the results showed the superiority of the neural network over nonlinear regression (Lim, 2005). Lim (2005) used a combination of artificial neural networks and genetic algorithms to estimate reservoir rock permeability in one of the wells based at an oil field in Korea that were used to estimate porosity in terms of polynomial functions. In this study, the aim was to optimize the coefficients of estimation polynomials, which, based on the above-mentioned combined method, better results were extracted than when artificial neural networks were used alone (Lim et al., 2006).

Al-Abduijabbar et al. (2020) developed an ANN method to estimate the reservoir porosity obtained from drilling operations. They used two different horizontal wells for training and validating the training data. They concluded that the ANN method would be a proper match to estimate porosity with approximately 30 neurons with a correlation coefficient of 0.907. In this paper, we resulted that ANN would be a good choice for porosity estimation, too (Al-Abduijabbar et al., 2020). It was developed by Okon et al. (2020) to use the ANN method to predict reservoir characteristics (Saikia et al., 2020). Saikia et al. (2020) presented a comprehensive review about the utilization of machine learning and ANN methods to predict reservoir characteristics such as porosity by implementing geophysical and geological resources. They reviewed that ANN methods should be combined with some hybrid models of soft computing to estimate reservoir characteristics regarding the complex nonlinear relationship between input and associated data in well logging processes. These models would be applicable and less time-consuming instead of well logging operations to determine reservoir characteristics (Okon et al., 2020).

The primary purpose of this study is to determine the porosity of Asmari reservoir rock in one of the oil fields located in the south of Iran using well patterns and well logs using neural phase networks. In this case, using the neural phase network technique is that despite drilling several wells in this field, in many of them, for various reasons, the most important of which is the high cost and time consuming to prepare the core, no coring has been done. However, to determine the exact characteristics of this field, the need for information at different depths of wells is felt. Therefore, using the neural network method to determine these parameters can be useful and a solution.

2. Materials and methods

Mansouri oilfield is located in the southwest of Iran, adjacent to Ahvaz and Shadegan oilfields. The sedimentary environment in different parts of this region is diverse, so that faces changes in Pabdeh, Asmari, Gachsaran, Mishan and Aghajari formations in this region have been detected (see Fig. 1).

In this paper, we are more focused on the Asmari formation. As the depths of the core data were not available, well data were not available, so they had to be interpolated based on data in their neighbourhood wells. These data were interpolated using Lagrange interpolation functions through programming that is performed in Matlab software. Due to the complexity of the geological conditions of the Asmari reservoir in Mansouri oilfield, six points in its vicinity were used to enter the data of well logs at any depth. These six points were symmetrical concerning the centre point. To help with the neural network training, the well logs are normalized. In this research, the input data were

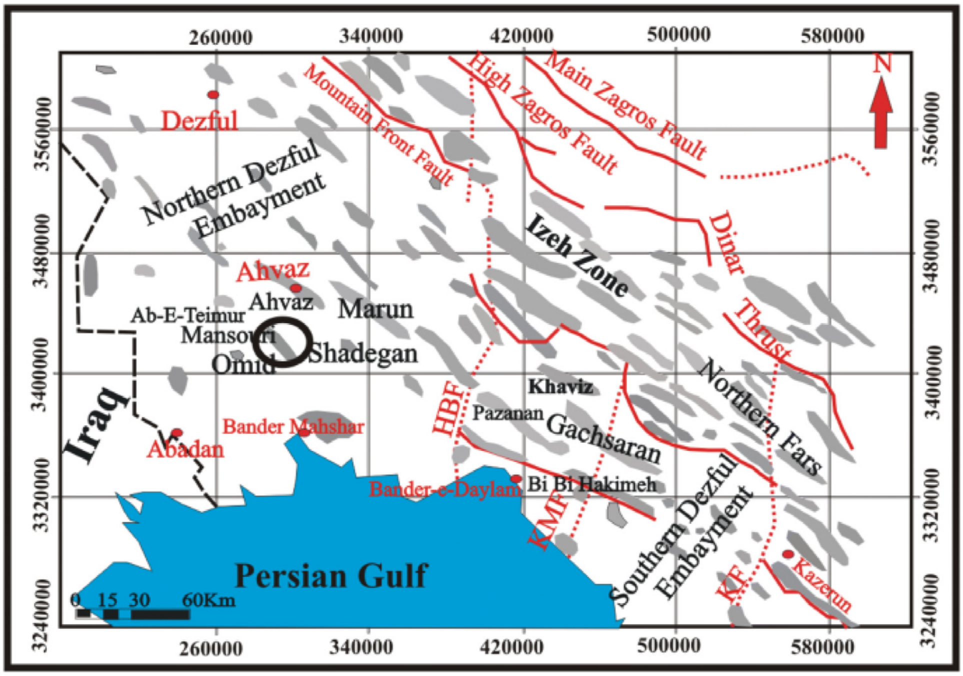

Fig. 1. Location of Mansouri oilfield.

normalized based on Eq. (1) and used in ANFIS neuro-phase network.

$$X_{Normalized} = \frac{X_i - X_{min}}{X_{max} - X_{min}} \tag{1}$$

Core porosity data are used in this study as both educational data and experimental data. These data for wells A, B and C have been prepared based on laboratory studies in the Petroleum Industry Research Institute using the mercury injection method. The number of core porosity data related to wells A, B and C are 150, 14 and 8 data, respectively, which is the same number of well image data generated by interpolation at the relevant depths.

- *Gaussian Shape Membership Function*

This function is defined as follows;

$$\Psi(x, \sigma, c) = Exp(-\frac{(x-c)^2}{2\sigma^2}) \tag{2}$$

As can be seen, σ and c are the two main parameters of this function.

- *Triangular Shape Membership Function*

This function is defined as follows;

$$\Psi(x, a, b, c) = \begin{Bmatrix} 0 & x \le c \\ \dfrac{x-a}{b-a} & a \le x \le b \\ \dfrac{c-x}{c-b} & b \le x \le c \\ 0 & x \ge c \end{Bmatrix} \tag{3}$$

This function depends on three variables a, b, c. The variables a, b show the base of this triangle, and the variable c shows its vertex.

- *Generalized Bell Shape Membership Function*

This function is defined as follows;

$$\Psi(x, a, b, c) = \frac{1}{1 + \left|\frac{x-c}{a}\right|^{2b}} \tag{4}$$

In this regard, the variable b is usually positive and shows the parameter c of the centre of the curve.

- *Trapezoidal Shape Membership Function*

This function is defined as follows;

$$\Psi(x, a, b, c, d) = \begin{Bmatrix} 0 & x \le c \\ \dfrac{x-a}{b-a} & a \le x \le b \\ 1 & b \le x \le c \\ \dfrac{d-x}{d-c} & c \le x \le d \\ 0 & x \ge d \end{Bmatrix} \tag{5}$$

In this regard, variables a, d shows the trapezoidal base and variables c, b show its shoulders. The membership functions are the same curves representing the fuzzy set. These functions assign each of the reference space X variables a degree of membership between [1 and 0]. Therefore, all functions that can receive values as input and generate output between [1 and 0] can be used as membership functions. These functions have different types, introduced in the following four examples of the most used ones.

3. Results and discussion

3.1. Selection of more effective logs in estimation by fuzzy log curves

In the case of multivariate functions, the effect of that variable on the function's output can be investigated by plotting the fuzzy curve of each variable. In any fuzzy curve where the amplitude of the output changes (Delta) is greater, it can be concluded that a variable such as this curve has a more influential role in controlling the answer of the function. In this paper, fuzzy curves were plotted for the data of natural acoustic gamma images, density, neutrons and diameters of wells A and B of the Mansouri field. Since short-range resistance and long-range resistance data were also available for well c, these data were plotted for these data, as well as data for five gamma, acoustic, neutron, and density logs. In these curves, the horizontal axis corresponds to the data of petrophysical logs, and the vertical axis indicates the porosity of the core at similar depths. These curves were plotted

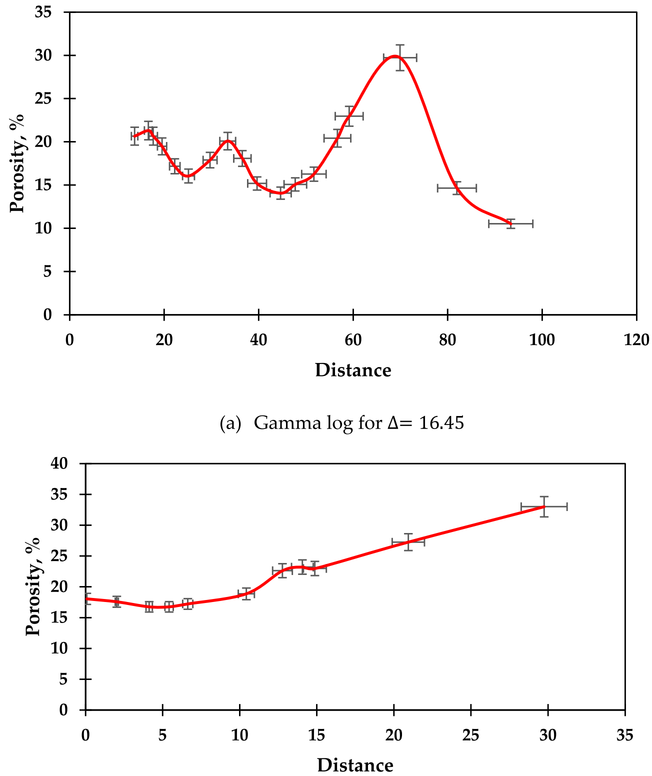

(a) Gamma log for Δ= 16.45

(b) Long-range resistance log for Δ= 14.125

Fig. 2. Gamma (a) and (b) long-range resistance logs.

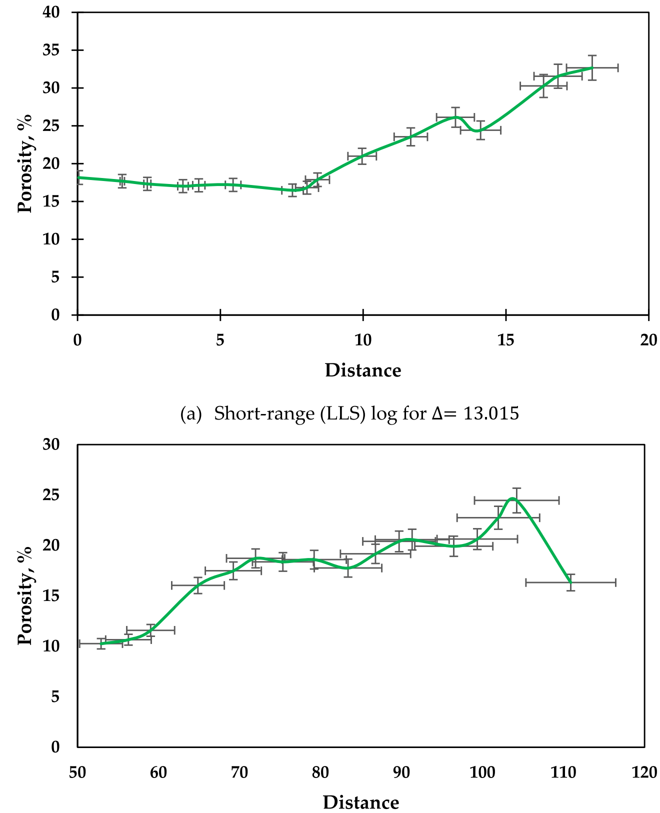

(a) Short-range (LLS) log for Δ= 13.015

(b) Acoustic resistance log for Δ= 10.951

Fig. 3. Short-range (a) and acoustic resistance (b) logs.

Table 1
Logs ranking and porosity ranges for well A.

Logs ranking	Log type	Porosity range
1	Gamma log	16.45
2	Long-range log	14.125
3	Short-range log	13.015
4	Acoustic resistance log	10.951
5	Density log	3.216
6	Neutron log	0.817
7	Diameter log	0.653

Table 2
Logs ranking and porosity ranges for well C.

Logs ranking	Log type	Porosity range
1	Gamma log	10.462
2	Acoustic resistance log	12.153
3	Density log	0.243
4	Neutron log	0.189
5	Diameter log	0.037

Table 3
Logs ranking and porosity ranges for well B.

Logs ranking	Log type	Porosity range
1	Gamma log	9.142
2	Acoustic resistance log	5.632
3	Density log	2.514
4	Neutron log	0.254
5	Diameter log	0.098

for the petrophysical graph data of well A through programming in Matlab environment, given below the shapes related to these curves and the following log rankings. The amplitude of porosity changes in these curves (Delta) for gamma images and long-range resistance are 16.45 and 14.125, respectively. It is shown in Fig. 2.

Fig. 3 shows these curves for short-range and acoustic resistance logs. The amplitude of porosity changes (Delta) in the curves related to these logs is 13.015 and 10.951, respectively.

These results are summarized in Table 1. In the image ranking column in this table, a lower-rated image plays a more influential role than a higher-ranked image in estimating porosity.

The fuzzy curves for well C of Mansouri Oilfield were plotted like well A. The amplitude of porosity changes is shown in Table 2 by ranking the petrophysical logs of well A in the estimation.

Fuzzy curves were also drawn for well B of Mansouri Oilfield. Table 3 shows the results of these curves by ranking the petrophysical logs of well B in the estimation.

Based on the results obtained from the fuzzy curves in the three wells A, B and C, the long-range resistance and short-range resistance logs are only available for well A, the gamma, acoustic, and density logs are, respectively. Neutrons and diameter measurements are used to estimate porosity in this field.

3.2. Select data for use in ANFIS software

ANFIS (adaptive-network-based fuzzy inference system) software is a fuzzy inference system to administer the frameworks of adaptive networks to model artificial neural networks. The purpose of designing a neuro-fuzzy network is to estimate porosity based on well graph data in different wells. Due to the complexity of the geological conditions of the Asmari reservoir in the Mansouri field and due to the need to cover the maximum output values by the training data set and the multiplicity of well A well data, we decided to mix the data of wells A and C. These data were used as neuro-phase network training data and well B data as experimental data to evaluate the ability of the neuro-phase

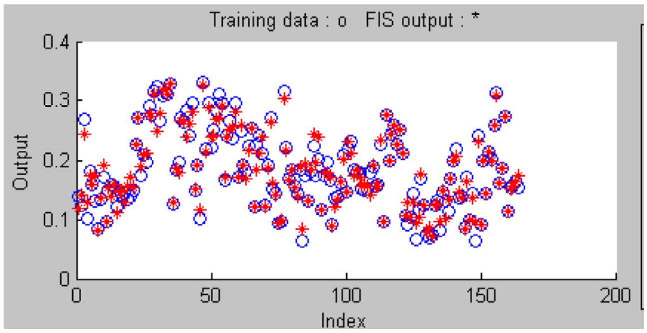

Fig. 4. Neuro-fuzzy network training based on the data of wells logs for wells A and C.

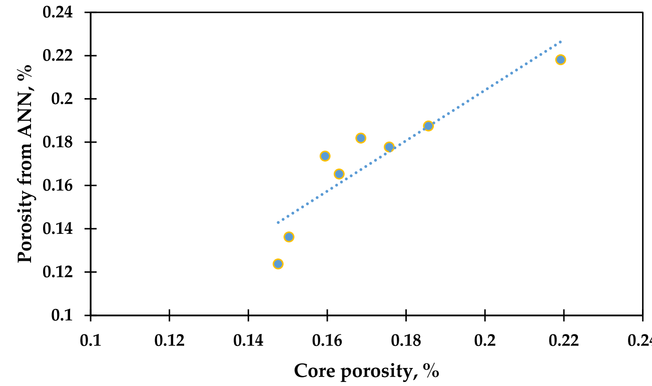

Fig. 5. The relationship between the porosity results obtained from the neuro-phase network.

Table 4
Porosity estimation for different logs (ANFIS software)

Log type	Gaussian membership number						
Gamma log	4	4	4	3	4	4	4
Acoustic log	2	2	2	2	1	2	2
Neutron log	2	2	2	2	2	2	1
Density log	3	2	1	1	1	1	1
Rules number	48	32	16	12	8	16	8
Training algorithm	H	B	B	B	B	H	H
Error percent	1.2	5.5	3.8	5.2	8.7	9.1	8.3

network in estimation after each training course. Therefore, the general model in estimation in this paper is based on this method.

3.3. Neuro-phase network architecture

Obtaining acceptable results in porosity estimation by intelligent neuro-fuzzy technique is related to the correct architecture of this network. This architecture includes selecting the appropriate type and number of membership functions to determine the degree of membership of input and output data and optimizing the network training in terms of the number of rules and network training algorithm. All the mentioned items can be changed and optimized through ANFIS software by trial and error method. In this research, the membership functions used for the input data are Gaussian, trapezoidal, triangular and bell-shaped membership functions. Linear and fixed membership functions have also been used to determine the degree of output membership. The educational algorithms in this research are based on post-diffusion and hybrid algorithms, which is a combination of post-diffusion algorithm and least oilfields. In this system, the output of each rule is obtained as a linear combination of input variables with a fixed sentence. The final output is a weighted average of the output of each rule. Since based on the fuzzy curves related to the well logs in three wells A, B and C, the barometer log was of the lowest importance due to the minimum amplitude of the changes (Delta), so the porosity estimation by the neural network with data of four Gamma, acoustic, density and neutron imaging were performed. The best results showed porosity estimation with a mean error of 1.28% and a correlation coefficient of 92.5% between the porosity of the core and the porosity resulting from the neural network in the validation data set in well B. These results are obtained by using four Gaussian membership functions for gamma graph data and two Gaussian membership functions for acoustic and density graph data, as well as three Gaussian membership functions for neutron graph data and assigning a linear membership function to the output and hybrid training algorithm. Was obtained. In this case, the number of fuzzy rules is 48 rules based on the Takagi–Sugeno fuzzy model.

These results are presented in Fig. 4 as the results of neuro-fuzzy network training based on wells logs for wells A and C and the test results based on wells B data. In this figure, the star-shaped points represent the results obtained from the neural network and the points in the form of hollow circles represent the input data.

Fig. 5 also shows the relationship between the porosity results obtained from the neuro-phase network versus the porosity of the core. Accordingly, the linear distribution of these points due to their high correlation coefficient represents an acceptable estimate by the neuro-phase network. Next, this optimal state of estimation is considered the base state, and the other cases are measured against it. In the estimation by the neuro-phase network, we seek to design a network with the least test error and the least number of neurons. Since the number of these neurons is directly related to the number of fuzzy laws, the number of neurons must be optimized by optimizing the number of fuzzy laws.

To optimize the number of fuzzy rules, the number of membership functions must be optimized. Since reducing the number of membership functions can reduce the number of fuzzy rules, tests were performed to evaluate the estimation in different cases in the recent neuro-fuzzy network. These modes include periodically subtracting the Gaussian membership function from the dedicated membership functions to gamma, acoustic, density, and neutron images in two training modes by the post-diffusion and hybrid algorithms. The results of these tests showed an increase in estimation error in all cases. These results are shown in Table 4. In the first column of this table, the baseline mode with the best estimation results is given. In the following columns of the table, we see a change in the number of dedicated membership functions to the graph data, followed by a change in the number of fuzzy rules, and finally, a change in the estimation error. In all cases of the test, the estimation error increases concerning the baseline. In these studies, the best estimation results are assigned by assigning four Gaussian membership functions to gamma image data.

Moreover, two Gaussian membership functions to each of the audio and neutron image data, and one Gaussian membership function to density image data and assigning a linear membership function. The output data were obtained by republishing using the educational algorithm and through 16 fuzzy rules. The average error in the validation data set in this case is 3.8%.

Based on this, the extent of the number of fuzzy rules can affect the estimation error. Similarly, increasing the number of membership functions associated with each input data can increase neurons and, consequently, increase the number of fuzzy rules and, in most cases, lead to the retention of training data by the neuro-fuzzy network. Despite these conditions, we will

Table 5
Porosity estimation for different training algorithms.

Ranking	Error percent	Rules number	Training algorithm	Function	Group number
1	1.2	40	H	Gaussian	1
2	6.8	32	P	trapezoidal	2
3	5.4	36	P	Gaussian	3

encounter many errors in estimating educational data. To get acquainted with assigning fuzzy rules to data by ANFIS software, these fuzzy rules for estimating porosity based on gamma, acoustic, neutron and density data and based on the best result of the estimation in Table 4 are brought. In this case, the dedicated membership functions to the image data are of the Gaussian type, and the linear membership function is assigned to the core porosity data.

3.4. Discussion

The results of the neuro-phase network in estimating the porosity are affected by the type of input data and the architecture of the neuro-phase network. To compare the performance of the data and the membership functions, and the training algorithm, these results are examined in different cases. First, the estimation results are presented based on different well logs. In the next step, in each of these groups, the role of membership functions and the training algorithm are presented in full detail. To compare the results of porosity estimation based on different logs, these estimation results were examined in three groups of four regarding the type of log. The first group included gamma, acoustic, density and neutron data and the second group included gamma, acoustic, neutron and spectroscopy data, and the third group included gamma, acoustic, density and densitometry data. In these studies, four Gaussian, trapezoidal, triangular and bell-shaped membership functions were assigned to the input data, and the linear membership function was assigned to the output. The results of these studies are given in Table 5.

4. Conclusion

As the ANN method gives a given appropriate descriptive data, intelligent techniques produce a fast and reliable prediction at a speed that appears to be a new set of data for model construction. The main findings of this study are as follows;

- The results of porosity estimation by intelligent neuro-phase method showed the ability of this method to estimate in complex conditions such as Mansouri field geological conditions in Asmari reservoir.
- The presence of raw data with appropriate accuracy plays a decisive role in estimation by the neuro-phase method.
- Preparing data before training the neural network increases the power of the network in recognizing the appropriate pattern.
- In cases where the neural network output is affected by multiple inputs, by fuzzy log curves, more effective inputs can be identified and used in network training.
- In estimating the porosity in the Asmari reservoir of Mansouri field, gamma, acoustic, neutron and density and diameter measurements have a more influential role.
- Selecting the appropriate architecture for the neuro-phase network is effective in achieving more accurate results. This architecture includes selecting the type and number of membership functions for the inputs and the training algorithm with the appropriate number of iteration steps.
- The best estimation results by assigning four Gaussian membership functions to gamma image data, two Gaussian membership functions to each of the audio and neutron data, and three Gaussian membership functions to density image data and creating 40 laws in the data space. Inputs were obtained using a hybrid training algorithm.
- The average error of estimating porosity by the neuro-phase method in well C of Mansouri field is 1.28% in the validation data set, representing a correlation coefficient of 92.5% between the porosity extracted from the fuzzy neuro-fuzzy network and the porosity of the core.

Nomenclature

LLS	Short-range resistance
LLD	Long-range resistance
ANN	Artificial neural network
x	Distance
σ	Tension
a	Constant parameter
b	Constant parameter
c	Constant parameter
H	Hybrid
B	Post diffusion
ANFIS	An adaptive-network-based fuzzy inference system

CRediT authorship contribution statement

Xiao Li: Methodology, Writing - original draft. **Bingxian Wang:** Investigation, Software, Writing - original draft. **Qiuyuan Hu:** Investigation. **Lis M. Yapanto:** Investigation, Validation. **Angelina Olegovna Zekiy:** Writing - review & editing.

Declaration of competing interest

The authors declare that they have no known competing financial interests or personal relationships that could have appeared to influence the work reported in this paper.

Acknowledgements

The National Nature Science and Technology Major Project of the Ministry of Science and Technology of China (No. 2016ZX05034-001).

References

Abasi, M., Razaz, M., Seifossadat, G., Moosapour, S., 2015. Presenting a new formulation to analyze and determine unbalance voltage produced at the place of load resulting from network and loads unbalance and asymmetry of transmission lines in radial power systems. Majlesi J. Energy Manage. 4 (3).

Abasi, M., Saffarian, A., Joorabian, M., Seifossadat, S.G., 2020. Fault location in double-circuit transmission lines compensated by generalized unified power flow controller (gupfc) based on synchronous current and voltage phasors. IEEE Syst. J..

Aggoun, R.C., Tiab, D., Owayed, J.F., 2006. Characterization of flow units in shaly sand reservoirs - Hassi R'mel Oil Rim, Algeria. J. Pet. Sci. Eng. https://doi.org/10.1016/j.petrol.2005.10.006.

Ahmadi, M.A., Ahmadi, M.R., Hosseini, S.M., Ebadi, M., 2014. Connectionist model predicts the porosity and permeability of petroleum reservoirs by means of petro-physical logs: Application of artificial intelligence. J. Pet. Sci. Eng. https://doi.org/10.1016/j.petrol.2014.08.026.

Aïfa, T., Baouche, R., Baddari, K., 2014. Neuro-fuzzy system to predict permeability and porosity from well log data: A case study of Hassi R'Mel gas field, Algeria. J. Pet. Sci. Eng. https://doi.org/10.1016/j.petrol.2014.09.019.

Al-Abduijabbar, A., Al-Azani, K., Elkatatny, S., 2020. Estimation of reservoir porosity from drilling parameters using artificial neural networks. Petrophysics https://doi.org/10.30632/PJV61N3-2020a5.

Awan, B., Sabeen, M., Shaheen, S., Mahmood, Q., Ebadi, A., Toughani, M., 2020. Phytoextraction of zinc contaminated water by Tagetes minuta L. Cent. Asian J. Environ. Sci. Technol. Innov. 1 (3), 150–158. https://doi.org/10.22034/CAJESTI.2020.03.04.

Bafkar, A., 2020. Kinetic and equilibrium studies of adsorptive removal of sodium-ion onto wheat straw and rice husk wastes. Cent. Asian J. Environ. Sci. Technol. Innov. 1 (6), https://doi.org/10.22034/CAJESTI.2020.06.04.

Baouche, R., Aïfa, T., 2017. Intelligent methods for predicting nuclear magnetic resonance of porosity and permeability by conventional well-logs: a case study of Saharan field. Arab. J. Geosci. https://doi.org/10.1007/s12517-017-3344-y.

Chen, Y., He, L., Guan, Y., Lu, H., Li, J., 2017. Life cycle assessment of greenhouse gas emissions and water-energy optimization for shale gas supply chain planning based on multi-level approach: Case study in Barnett, Marcellus, Fayetteville, and Haynesville shales. Energy Convers. Manage. https://doi.org/10.1016/j.enconman.2016.12.019.

Chen, Y., He, L., Li, J., Zhang, S., 2018. Multi-criteria design of shale-gas-water supply chains and production systems towards optimal life cycle economics and greenhouse gas emissions under uncertainty. Comput. Chem. Eng. https://doi.org/10.1016/j.compchemeng.2017.11.014.

Chen, X., Wang, D. yong, Tang, J. bin, Ma, W. chen, Liu, Y., 2021. Geotechnical stability analysis considering strain softening using micro-polar continuum finite element method. J. Cent. South Univ. https://doi.org/10.1007/s11771-021-4603-3.

Cheng, X., He, L., Lu, H., Chen, Y., Ren, L., 2016. Optimal water resources management and system benefit for the Marcellus shale-gas reservoir in Pennsylvania and West Virginia. J Hydrol. https://doi.org/10.1016/j.jhydrol.2016.06.041.

Daryayehsalameh, B., Nabavi, M., Vaferi, B., 2021. Modeling of co_2 capture ability of [bmim][bf4] ionic liquid using connectionist smart paradigms. Environ. Technol. Innov. 22, 101484.

Davarpanah, A., 2018a. Feasible analysis of reusing flowback produced water in the operational performances of oil reservoirs. Environ. Sci. Pollut. Res. https://doi.org/10.1007/s11356-018-3506-9.

Davarpanah, A., 2018b. A feasible visual investigation for associative foam >\ polymer injectivity performances in the oil recovery enhancement. Eur. Polym. J. https://doi.org/10.1016/j.eurpolymj.2018.06.017.

Davarpanah, A., 2019. The feasible visual laboratory investigation of formate fluids on the rheological properties of a shale formation. Int. J. Environ. Sci. Technol. https://doi.org/10.1007/s13762-018-1877-6.

Davarpanah, A., 2020. Parametric study of polymer-nanoparticles-assisted injectivity performance for axisymmetric two-phase flow in EOR processes. Nanomaterials https://doi.org/10.3390/nano10091818.

Davarpanah, A., Mazarei, M., Mirshekari, B., 2019a. A simulation study to enhance the gas production rate by nitrogen replacement in the underground gas storage performance. Energy Rep. https://doi.org/10.1016/j.egyr.2019.04.004.

Davarpanah, A., Mirshekari, B., 2018. A simulation study to control the oil production rate of oil-rim reservoir under different injectivity scenarios. Energy Rep. https://doi.org/10.1016/j.egyr.2018.10.011.

Davarpanah, A., Mirshekari, B., 2019a. Experimental investigation and mathematical modeling of gas diffusivity by carbon dioxide and methane kinetic adsorption. Ind. Eng. Chem. Res. https://doi.org/10.1021/acs.iecr.9b01920.

Davarpanah, A., Mirshekari, B., 2019b. Experimental study of CO<inf>2</inf> solubility on the oil recovery enhancement of heavy oil reservoirs. J. Therm. Anal. Calorim. https://doi.org/10.1007/s10973-019-08498-w.

Davarpanah, A., Mirshekari, B., 2019c. A mathematical model to evaluate the polymer flooding performances. Energy Rep. https://doi.org/10.1016/j.egyr.2019.09.061.

Davarpanah, A., Mirshekari, B., 2019d. Mathematical modeling of injectivity damage with oil droplets in the waste produced water re-injection of the linear flow. Eur. Phys. J. Plus. https://doi.org/10.1140/epjp/i2019-12546-9.

Davarpanah, A., Mirshekari, B., 2020. Numerical simulation and laboratory evaluation of alkali–surfactant–polymer and foam flooding. Int. J. Environ. Sci. Technol. https://doi.org/10.1007/s13762-019-02438-9.

Davarpanah, A., Mirshekari, B., Jafari Behbahani, T., Hemmati, M., 2018. Integrated production logging tools approach for convenient experimental individual layer permeability measurements in a multi-layered fractured reservoir. J. Pet. Explor. Prod. Technol. https://doi.org/10.1007/s13202-017-0422-3.

Davarpanah, A., Shirmohammadi, R., Mirshekari, B., 2019c. Experimental evaluation of polymer-enhanced foam transportation on the foam stabilization in the porous media. Int. J. Environ. Sci. Technol. https://doi.org/10.1007/s13762-019-02280-z.

Davarpanah, A., Shirmohammadi, R., Mirshekari, B., Aslani, A., 2019b. Analysis of hydraulic fracturing techniques: hybrid fuzzy approaches. Arab. J. Geosci. https://doi.org/10.1007/s12517-019-4567-x.

Ebadati, A., Akbari, E., Davarpanah, A., 2019a. An experimental study of alternative hot water alternating gas injection in a fractured model. Energy Explor. Exploit. 37 (3), 945–959.

Ebadati, A., Davarpanah, A., Shahhoseini, A., Ahmadi, P., 2019b. An experimental study to measure the required fresh water and treated water for drilling an unconventional shale reservoir. Int. J. Environ. Sci. Technol. https://doi.org/10.1007/s13762-018-02185-3.

Ebadi, A., Toughani, M., Najafi, A., Babaee, M., 2020. A brief overview on current environmental issues in Iran. Cent. Asian J. Environ. Sci. Technol. Innov. 1 (1), 1–11. https://doi.org/10.22034/CAJESTI.2020.01.08.

Elsharkawy, A.M., 1998. Modeling the properties of crude oil and gas systems using RBF network. In: SPE - Asia Pacific Oil Gas Conf. https://doi.org/10.2523/49961-ms.

Esfandyari, H., Haghighat Hoseini, A., Shadizadeh, S.R., Davarpanah, A., 2020a. Simultaneous evaluation of capillary pressure and wettability alteration based on the USBM and imbibition tests on carbonate minerals. J Pet Sci Eng. https://doi.org/10.1016/j.petrol.2020.108285.

Esfandyari, H., Shadizadeh, S.R., Esmaeilzadeh, F., Davarpanah, A., 2020b. Implications of anionic and natural surfactants to measure wettability alteration in EOR processes. Fuel https://doi.org/10.1016/j.fuel.2020.118392.

Ghiasi-Freez, J., Ziaii, M., Kadkhodaie-Ilkhchi, A., Honarmand, J., 2014. A reservoir rock porosity estimation through image analysis and fuzzy logic techniques. Energy Sources Part A Recover. Util. Environ. Eff. https://doi.org/10.1080/15567036.2011.574198.

Gholami, A., Ansari, H.R., 2017. Estimation of porosity from seismic attributes using a committee model with bat-inspired optimization algorithm. J. Pet. Sci. Eng. https://doi.org/10.1016/j.petrol.2017.03.013.

Hassanpour, A., Farhami, N., Derakhshande, M., Nezhad, P.D.K., Ebadi, A., Ebrahimiasl, S., 2021. Magnesium and calcium ion batteries based on the hexa-peri-hexabenzocoronene nanographene anode materials. Inorg. Chem. Commun. 108656. https://doi.org/10.1016/j.inoche.2021.108656.

He, L., Chen, Y., Li, J., 2018b. A three-level framework for balancing the tradeoffs among the energy, water, and air-emission implications within the life-cycle shale gas supply chains. Resour. Conserv. Recy. https://doi.org/10.1016/j.resconrec.2018.02.015.

He, L., Chen, Y., Zhao, H., Tian, P., Xue, Y., Chen, L., 2018a. Game-based analysis of energy-water nexus for identifying environmental impacts during Shale gas operations under stochastic input. Sci Total Environ. https://doi.org/10.1016/j.scitotenv.2018.02.004.

Hu, X., Xie, J., Cai, W., Wang, R., Davarpanah, A., 2020. Thermodynamic effects of cycling carbon dioxide injectivity in shale reservoirs. J. Pet. Sci. Eng. https://doi.org/10.1016/j.petrol.2020.107717.

Huang, J., Duan, T., Zhang, Y., Liu, J., Zhang, J., Lei, Y., 2020a. Predicting the permeability of pervious concrete based on the beetle antennae search algorithm and random forest model. Adv. Civil Eng. https://doi.org/10.1155/2020/8863181.

Huang, K., Ge, S., 2020. The anti-CXCL4 antibody depletes CD4(+)CD25(+)FOXP3(+) regulatory T cells from CD4+ T cells from chronic osteomyelitis patients by the STAT5 pathway. Ann. Cardiothorac. Surg. https://doi.org/10.21037/apm-20-166.

Huang, J., Kumar, G.S., Sun, Y., 2021b. Evaluation of workability and mechanical properties of asphalt binder and mixture modified with waste toner. Constr. Building Mater. 276, 122230. https://doi.org/10.1016/j.conbuildmat.2020.122230.

Huang, J., Shiva Kumar, G., Ren, J., Sun, Y., Li, Y., Wang, C., 2021a. Towards the potential usage of eggshell powder as bio-modifier for asphalt binder and mixture: workability and mechanical properties. Internat. J. Pavement Eng. 1–13.

Huang, J., Sun, Y., Zhang, J., 2021c. Reduction of computational error by optimizing SVR kernel coefficients to simulate concrete compressive strength through the use of a human learning optimization algorithm. Eng. Comput. 1–18.

Huang, J., Wang, Q.A., 2021. Influence of crumb rubber particle sizes on rutting. low temperature cracking, fracture, and bond strength properties of asphalt binder 54 (2), 1–15. https://doi.org/10.1617/s11527-021-01647-4.

Huang, J., Zhang, J., Ren, J., Chen, H., 2021d. Anti-rutting performance of the damping asphalt mixtures (DAMs) made with a high content of asphalt rubber (AR). Construct. Build. Mater. 271, 121878. https://doi.org/10.1016/j.conbuildmat.2020.121878.

Huang, J., Zhang, Y., Sun, Y., Ren, J., Zhao, Z., Zhang, J., 2021e. Evaluation of pore size distribution and permeability reduction behavior in pervious concrete. Constr. Build. Mater. 290, 123228. https://doi.org/10.1016/j.conbuildmat.2021.123228.

Huang, C., Zheng, Y., Lin, W., Shi, Y., Huang, G., Yong, Q., 2020b. Removal of fermentation inhibitors from pre-hydrolysis liquor using polystyrene divinylbenzene resin. Biotechnol. Biofuels https://doi.org/10.1186/s13068-020-01828-3.

Jafarinezhad, S., Shahbazian, M., 2015. Modeling the porosity of the carbonate reservoir using a genetic type-2 fuzzy logic system. Energy Sources Part A Recover. Util. Environ. Eff. https://doi.org/10.1080/15567036.2011.574196.

Jalali Sarvestani, M., Charehjou, P., 2021. Fullerene (C20) as a potential adsorbent and sensor for the removal and detection of picric acid contaminant: DFT studies. Cent. Asian J. Environ. Sci. Technol. Innov. 2 (1), https://doi.org/10.22034/CAJESTI.2021.01.02.

Jiang, Q., Shao, F., Lin, W., Gu, K., Jiang, G., Sun, H., 2018. Optimizing multistage discriminative dictionaries for blind image quality assessment. IEEE Trans Multimed. https://doi.org/10.1109/TMM.2017.2763321.

Karbakhshzadeh, A., Derakhshande, M., Farhami, N., Hosseinian, A., Ebrahimi-asl, S., Ebadi, A., 2021a. Study the adsorption of letrozole drug on the silicon doped graphdiyne monolayer: a dft investigation. Silicon 1–8. https://doi.org/10.1007/s12633-021-01143-y.

Karbakhshzadeh, A., Heravi, M.R.P., Rahmani, Z., Ebadi, A., Vessally, E., 2021b. Aroyl fluorides: novel and promising arylating agents. J. Fluor. Chem. 109806. https://doi.org/10.1016/j.jfluchem.2021.109806.

Kargar, P., Osouli, A., Vaughn, B., Hosseini, A., Rostami, H., 2020. Feasibility study of collapse remediation of illinois loess using electrokinetics technique by nanosilica and salt. https://doi.org/10.1061/9780784482780.066.

Kartavykh, S., Komandyrov, O., Kulikov, P., Ploskyi, V., Poltorachenko, N., Terenchuk, S., 2020. Adaptation of fuzzy inference system to solve assessment problems of technical condition of construction objects. Technol. Audit. Prod Reserv. https://doi.org/10.15587/2706-5448.2020.205364.

Kazemi, A., Yang, S., 2019. Atomistic study of the effect of magnesium dopants on the strength of nanocrystalline aluminum. JOM https://doi.org/10.1007/s11837-019-03373-3.

Kazemi, A., Yang, S., 2021. Effects of magnesium dopants on grain boundary migration in aluminum-magnesium alloys. Comput. Mater. Sci. https://doi.org/10.1016/j.commatsci.2020.110130.

Lee, S., Jung, S., Lee, J., 2019. Prediction model based on an artificial neural network for user-based building energy consumption in South Korea. Energies https://doi.org/10.3390/en12040608.

Li, Y., Jia, D., Rui, Z., Peng, J., Fu, C., Zhang, J., 2017. Evaluation method of rock brittleness based on statistical constitutive relations for rock damage. J. Pet. Sci. Eng. https://doi.org/10.1016/j.petrol.2017.03.041.

Li, Y., Long, M., Tang, J., Chen, M., Fu, X., 2020. A hydraulic fracture height mathematical model considering the influence of plastic region at fracture tip. Pet. Explor. Dev. https://doi.org/10.1016/S1876-3804(20)60017-9.

Li, Y., Long, M., Zuo, L., Li, W., Zhao, W., 2019. Brittleness evaluation of coal based on statistical damage and energy evolution theory. J. Pet. Sci. Eng. https://doi.org/10.1016/j.petrol.2018.08.069.

Lim, J.S., 2005. Reservoir properties determination using fuzzy logic and neural networks from well data in offshore Korea. J. Pet. Sci. Eng. https://doi.org/10.1016/j.petrol.2005.05.005.

Lim, J.S., Park, H.J., Kim, J., 2006. A new neural network approach to reservoir permeability estimation from well logs. In: Proc - SPE Asia Pacific Oil Gas Conf Exhib 2006 Thriving Volatility. https://doi.org/10.2523/100989-ms.

Lin, W., Xing, S., Jin, Y., Lu, X., Huang, C., Yong, Q., 2020. Insight into understanding the performance of deep eutectic solvent pretreatment on improving enzymatic digestibility of bamboo residues. Bioresour. Technol. https://doi.org/10.1016/j.biortech.2020.123163.

Ma, X., Zhang, K., Zhang, L., Yao, C., Yao, J., Wang, H., Jian, W., Yan, Y., 2021. Data-driven niching differential evolution with adaptive parameters control for history matching and uncertainty quantification. SPE J. https://doi.org/10.2118/205014-pa.

Maina, Y., Kyari, B., Jimme, M., 2020. Impact of household fuel expenditure on the environment: the quest for sustainable energy in Nigeria. Cent. Asian J. Environ. Sci. Technol. Innov. 1 (2), 109–118. https://doi.org/10.22034/CAJESTI.2020.02.06.

Mao, Q.-F., Shang-Guan, Z.-F., Chen, H.-L., Huang, K., 2019. Immunoregulatory role of IL-2/STAT5/CD4+CD25+Foxp3 Treg pathway in the pathogenesis of chronic osteomyelitis. Ann Transl. Med. https://doi.org/10.21037/atm.2019.07.45.

Mazarei, M., Davarpanah, A., Ebadati, A., Mirshekari, B., 2019. The feasibility analysis of underground gas storage during an integration of improved condensate recovery processes. J. Pet. Explor. Prod. Technol. https://doi.org/10.1007/s13202-018-0470-3.

Movahhed, A., Bidhendi, M.N., Masihi, M., Emamzadeh, A., 2019. Introducing a method for calculating water saturation in a carbonate gas reservoir. J. Nat. Gas. Sci. Eng. https://doi.org/10.1016/j.jngse.2019.102942.

Najafi, M., Najafi, M., Najafi, H., 2012. DFT/B3LYP study of the substituent effects on the reaction enthalpies of the antioxidant mechanisms of indole-3-carbinol derivatives in the gas-phase and water. Comput. Theor. Chem. https://doi.org/10.1016/j.comptc.2012.08.008.

Najafi, M., Najafi, M., Najafi, H., 2013. Theoretical study of the substituent effects on the reaction enthalpies of the antioxidant mechanisms of stobadine derivatives in the gas-phase and water. J. Theor. Comput. Chem. https://doi.org/10.1142/S0219633612501167.

Nan, S., Hai-Bin, W., Li, G., Jing-Yao, Z., Jian-Feng, G., Fang, W., Ebadi, A., 2021. Sila-, bora-, thio-, and phosphono-carboxylation of unsaturated compounds with carbon dioxide: an overview. J. CO_2 Utiliz. 48, 101522. https://doi.org/10.1016/j.jcou.2021.101522.

Nnaemeka, A., 2020. Environmental pollution and associated health hazards to host communities (case study: Niger delta region of Nigeria). Cent. Asian J. Environ. Sci. Technol. Innov. 1 (1), 30–42. https://doi.org/10.22034/CAJESTI.2020.01.04.

Nwankwo, C., E. Gobo, A., Israel-Cookey, C., A. Abere, S., 2020. Effects of hazardous waste discharge from the activities of oil and gas companies in Nigeria. Cent. Asian J. Environ. Sci. Technol. Innov. 1 (2), 119–129. https://doi.org/10.22034/CAJESTI.2020.02.07.

Okon, A.N., Adewole, S.E., Uguma, E.M., 2020. Artificial neural network model for reservoir petrophysical properties: porosity, permeability and water saturation prediction. Model. Earth Syst. Environ. 26, 1–8.

Pan, F., Zhang, Z., Zhang, X., Davarpanah, A., 2020. Impact of anionic and cationic surfactants interfacial tension on the oil recovery enhancement. Powder Technol. https://doi.org/10.1016/j.powtec.2020.06.033.

Qayyum, S., Khan, I., Meng, K., Zhao, Y., Peng, C., 2020. A review on remediation technologies for heavy metals contaminated soil. Cent. Asian J. Environ. Sci. Technol. Innov. 1 (1), 21–29. https://doi.org/10.22034/CAJESTI.2020.01.03.

Rabbani, E., Davarpanah, A., Memariani, M., 2018. An experimental study of acidizing operation performances on the wellbore productivity index enhancement. J. Pet. Explor. Prod. Technol. https://doi.org/10.1007/s13202-018-0441-8.

Rezaee, M., Kargar Ghomeshe, P., Mohammad Hosseini, A., 2017. Electrokinetic remediation of zinc and copper contaminated soil: A simulation-based study. Civ. Eng. J. https://doi.org/10.21859/cej-03096.

Rostami, Z., Asnaashariisfahani, M., Ahmadi, S., Hosseinian, A., Ebadi, A., 2021. A density functional theory investigation on 1h-4-germapyridine-4-ylidene & the unsaturated heterocyclic substituted ones. J. Molecular Struct. 1238, 130427. https://doi.org/10.1016/j.molstruc.2021.130427.

Saikia, P., Baruah, R.D., Singh, S.K., Chaudhuri, P.K., 2020. Artificial neural networks in the domain of reservoir characterization: A review from shallow to deep models. Comput. Geosci. https://doi.org/10.1016/j.cageo.2019.104357.

Sepahvand, T., Etemad, V., Matinizade, M., Shirvany, A., 2021a. Symbiosis of AMF with growth modulation and antioxidant capacity of Caucasian Hackberry (Celtis Caucasica L.) seedlings under drought stress. Cent. Asian J. Environ. Sci. Technol. Innov. 2 (1), https://doi.org/10.22034/CAJESTI.2021.01.03.

Sharma, M., Garg, R., 2020. An artificial neural network based approach for energy efficient task scheduling in cloud data centers. Sustain. Comput. Inform. Syst. https://doi.org/10.1016/j.suscom.2020.100373.

Shokir, E.M.E.M., 2006. A novel model for permeability prediction in uncored wells. SPE Reserv. Eval. Eng. https://doi.org/10.2118/87038-pa.

Singh, S., 2005. Permeability prediction using artificial neural network (ANN): A case study of Uinta Basin. In: Proc - SPE Annu Tech Conf Exhib. https://doi.org/10.2118/99286-stu.

Sun, S., Zhou, M., Lu, W., Davarpanah, A., 2020. Application of symmetry law in numerical modeling of hydraulic fracturing by finite element method. Symmetry (Basel) https://doi.org/10.3390/sym12071122.

Valipour, M., Banihabib, M.E., Behbahani, S.M.R., 2012. Monthly inflow forecasting using autoregressive artificial neural network. J. Appl. Sci. https://doi.org/10.3923/jas.2012.2139.2147.

Wang, J., Kim, Y.H., Ryu, J., Jeong, C., Choi, W., Kim, D., 2021. Artificial neural network-based compact modeling methodology for advanced transistors. IEEE Trans. Electron Devices https://doi.org/10.1109/TED.2020.3048918.

Wang, X., Yang, S., Wang, Y., Zhao, Y., Ma, B., 2019. Improved permeability prediction based on the feature engineering of petrophysics and fuzzy logic analysis in low porosity–permeability reservoir. J. Pet. Explor. Prod. Technol. https://doi.org/10.1007/s13202-018-0556-y.

Wawrzyniak, J., 2020. Application of artificial neural networks to assess the mycological state of bulk stored rapeseeds. Agric. https://doi.org/10.3390/agriculture10110567.

Xu, J., Li, Y., Ren, C., Wang, S., Vanapalli, S.K., Chen, G., 2021. Influence of freeze-thaw cycles on microstructure and hydraulic conductivity of saline intact loess. Cold Reg. Sci. Technol. https://doi.org/10.1016/j.coldregions.2020.103183.

Xue, X., Zhang, K., Tan, K.C., Feng, L., Wang, J., Chen, G., Zhao, X., Zhang, L., Yao, J., 2020. Affine transformation-enhanced multifactorial optimization for heterogeneous problems. IEEE Trans. Cybern. https://doi.org/10.1109/TCYB.2020.3036393.

Yang, Y., Li, Y., Yao, J., Iglauer, S., Luquot, L., Zhang, K., Sun, H., Zhang, L., Song, W., Wang, Z., 2020a. Dynamic pore-scale dissolution by CO2-saturated brine in carbonates: Impact of homogeneous versus fractured versus vuggy pore structure. Water Resour. Res. 56 (4), https://doi.org/10.1029/2019WR026112.

Yang, Y., Tao, L., Yang, H., Iglauer, S., Wang, X., Askari, R., et al., 2020b. Stress sensitivity of fractured and vuggy carbonate: An X-ray computed tomography analysis. J. Geophys. Res. Solid Earth. 125], number=3,, https://doi.org/10.1029/2019JB018759.

Yang, Y., Yao, J., Wang, C., Gao, Y., Zhang, Q., An, S., Song, W., 2015. New pore space characterization method of shale matrix formation by considering organic and inorganic pores. J. Nat. Gas Sci. Eng. https://doi.org/10.1016/j.jngse.2015.08.017.

Yin, F., Xue, X., Zhang, C., Zhang, K., Han, J., Liu, B., et al., 2021. Multifidelity genetic transfer: an efficient framework for production optimization. SPE J. 1–22. https://doi.org/10.2118/205013-PA.

Zarra, T., Galang, M.G., Ballesteros, F., Belgiorno, V., Naddeo, V., 2019. Environmental odour management by artificial neural network – a review. Environ. Int. https://doi.org/10.1016/j.envint.2019.105189.

Zhang, F., An, M., Zhang, L., Fang, Y., Elsworth, D., 2020a. Effect of mineralogy on friction-dilation relationships for simulated faults: Implications for permeability evolution in caprock faults. Geosci. Front. https://doi.org/10.1016/j.gsf.2019.05.014.

Zhang, K., Jia, C., Song, Y., Jiang, S., Jiang, Z., Wen, M., Liu, T., 2020b. Analysis of lower cambrian shale gas composition, source and accumulation pattern in different tectonic backgrounds: a case study of weiyuan block in the upper yangtze region and Xiuwu Basin in the lower Yangtze region. Fuel (Guildford) 263, 115978. https://doi.org/10.1016/j.fuel.2019.115978.

Zhang, K., Zhang, J., Ma, X., Yao, C., Zhang, L., Yang, Y., Wang, J., Yao, J., Zhao, H., 2021. History matching of naturally fractured reservoirs using a deep sparse autoencoder. SPE J. https://doi.org/10.2118/205340-pa.

Zheng, Y., Yu, Y., Lin, W., Jin, Y., Yong, Q., Huang, C., 2021a. Enhancing the enzymatic digestibility of bamboo residues by biphasic phenoxyethanol-acid pretreatment. Bioresour. Technol. https://doi.org/10.1016/j.biortech.2021.124691.

Zheng, L., Yu, P., Zhang, Y., Wang, P., Yan, W., Guo, B., Huang, C., Jiang, Q., 2021b. Evaluating the bio-application of biomacromolecule of lignin-carbohydrate complexes (LCC) from wheat straw in bone metabolism via ROS scavenging. Int. J. Biol. Macromol. https://doi.org/10.1016/j.ijbiomac.2021.01.103.

Zhou, C.D., Wu, X.L., Cheng, J.A., 1993. Determining reservoir properties in reservoir studies using a fuzzy neural network. In: Proc - SPE Annu Tech Conf Exhib. https://doi.org/10.2523/26430-ms.

Zhu, M., Yu, L., Zhang, X., Davarpanah, A., 2020. Application of implicit pressure-explicit saturation method to predict filtrated mud saturation impact on the hydrocarbon reservoirs formation damage. Mathematics https://doi.org/10.3390/MATH8071057.

Zuo, C., Chen, Q., Tian, L., Waller, L., Asundi, A., 2015. Transport of intensity phase retrieval and computational imaging for partially coherent fields: The phase space perspective. Opt. Lasers Eng. https://doi.org/10.1016/j.optlaseng.2015.03.006.

Zuo, C., Sun, J., Li, J., Zhang, J., Asundi, A., Chen, Q., 2017. High-resolution transport-of-intensity quantitative phase microscopy with annular illumination. Sci. Rep. https://doi.org/10.1038/s41598-017-06837-1.